Particle Size and Monomer Partitioning in Microemulsion Polymerization. 2. Online Small Angle Neutron Scattering Studies

Carlos C. Co and Eric W. Kaler*

Center for Molecular and Engineering Thermodynamics, Department of Chemical Engineering, University of Delaware, Newark, Delaware 19716

Received November 21, 1997; Revised Manuscript Received March 2, 1998

ABSTRACT: Polymerization of *n*-hexyl methacrylate (C_6MA) in aqueous microemulsions made with mixed dodecyltrimethylammonium bromide (DTAB) and didodecyldimethylammonium bromide (DDAB) surfactants yields very small (∼30 nm) latex particles of high molecular weight polymer. The results of an online small-angle neutron scattering (SANS) experiment have verified some of the assumptions of a simple but accurate kinetic model that has been recently proposed for aqueous microemulsion polymerization. The SANS results also support the predictions of an analytical model that describes the evolution of the chain length and particle size distribution throughout the polymerization. During the microemulsion polymerization of C_6MA, the monomer does not significantly swell the polymer particles. A model of the reacting particle as a polymer core surrounded by a monomer-rich shell is consistent with both the kinetic and SANS data if the monomer concentration in the shell is equal to that in the core of the swollen micelles

1. Introduction

Microemulsion and conventional emulsion polymerizations appear to be similar, but the underlying mechanisms are different. In contrast to emulsion polymerization, large monomer droplets are never present in a microemulsion and monomer-containing micelles (which present a very large interfacial area) are initiated throughout microemulsion polymerization by radical entry to form polymer particles. These important differences were accounted for and used by Morgan et al.[1] in developing a kinetic model based on the novel assumptions of rapid entry of aqueous free radicals and negligible biradical termination. This model predicts quantitatively the polymerization kinetics of *n*-hexyl methacrylate (C_6MA) in aqueous microemulsions made with mixed dodecyltrimethylammonium bromide (DTAB) and didodecyldimethylammonium bromide (DDAB) surfactants. The phase behavior and microstructure of these microemulsions have been well characterized and reported elsewhere.[2,3]

As in all polymerization kinetic models, it is necessary to relate the monomer concentration at the locus of polymerization to monomer conversion. This requires some care for compartmentalized emulsion and microemulsion polymerization reactions where the monomer can partition between two or more domains or phases. In emulsion polymerization, monomer partitioning between the large emulsion droplets and growing polymer particles depends strongly on the interfacial tension and interactions between the polymer and monomer. Diffusion of monomer from the emulsion droplets to the growing polymer particles is rapid and equilibrium partitioning is usually assumed. Gilbert[4] has summarized some experimental methods used to determine the equilibrium monomer concentration in polymer particles during emulsion polymerization.

A thermodynamic model has been developed to describe the polymerization of styrene in a specific microemulsion.[5,6] The partitioning of the styrene monomer in the oil, interface, aqueous, and polymer pseudophases is calculated using a Flory−Huggins type approach. The model predicts that essentially all of the monomer is taken up by the nascent polymer particles at low conversions (∼5%), and the concentration of monomer at the site of polymerization then decreases approximately linearly afterward with conversion. This favorable partitioning of monomer to swell the polymer is a consequence of the value of the Flory parameter used to characterize the interaction between styrene and polystyrene.

In the other limit in which monomer does not partition into the polymer, the growing polymer particles would consist of a compact polymer core and an interface or shell of monomer diluted by the hydrocarbon tails of the adsorbed surfactant.[1] The locus of polymerization would then be in the shell of monomer and surfactant tails where the monomer concentration can be assumed to be the same as that in the core of the monomer swollen micelles. In this case, the monomer concentration also decreases approximately linearly with conversion, but most of the monomer is partitioned into the micelles.

For both of the two limiting cases (monomer/polymer mixing or segregation) there is a linear relationship between the monomer concentration at the locus of polymerization (c) and the conversion (f), so that the expression, $c = c_o(1 - f)$ is approximately valid for both cases. Therefore, kinetic measurements alone cannot readily distinguish between these two mechanisms. In the case of complete monomer/polymer segregation, the value of c_o will be the molar concentration of monomer in the micelle cores of the unpolymerized microemulsion. This value can be calculated from the known monomer and surfactant hydrocarbon tail volumes. In the other case of uniform monomer/polymer mixing, c_o depends on the degree of conversion at which sufficient polymer has formed to absorb all available monomer and must be calculated from a thermodynamic model. In either case, this linear approximation leads to a kinetic model,

* To whom correspondence should be addressed.

S0024-9297(97)01718-X CCC: $15.00
Published on Web 04/23/1998

the chief result of which is the simple expression for conversion as a function of time,[1]

$$f = 1 - \exp\left(-\frac{1}{2}At^2\right) \quad (1)$$

where $A = 2k_dk_pc_o[I]/M_o$. Here k_d and k_p are the initiator decomposition and monomer propagation rate constants, and [I] and M_o are the initiator and monomer concentration in the entire microemulsion. The value of c_o can be obtained from experimental kinetic data if k_d and k_p are known accurately. For C_6MA microemulsion polymerization, a value of c_o corresponding to the case of complete monomer/polymer segregation was found to be consistent with the experimental kinetic data given the uncertainties in the rate constants.[1]

In the first paper of this series (paper 1), a new technique for calculating the particle size distribution during microemulsion polymerization is described in detail. In particular, an analytical equation describing the evolution of the chain length distribution during microemulsion polymerization is derived, for the limiting case of no radical exit, based on the same mechanistic ideas embodied in the kinetic model described above. The expression for the growth rate of a single chain is used to determine (1) the previous time (t_1) when a chain must be initiated to grow to a length of L monomer units at time t, and (2) the time period necessary for one propagation event at time t_1. The number of chains initiated in this time period at time t_1 is then equal to the number of chains with length L at time t. However, in typical microemulsion polymerization systems, chain transfer to monomer followed by radical exit from the growing particle appears to be the dominant mechanism for chain termination. To account for this, the latter model was supplemented with chain transfer probabilities to give an analytical equation that describes the particle size distribution in the limit of transfer-controlled exit. The particle size distribution is readily obtained from the chain-length distribution model if the monomer does not mix or swell the polymer particles and if each particle contains only a single chain. This will be the case if the growing particles do not coalesce and if chain transfer to monomer leads predominantly to radical exit from the growing particle.

In this paper, we present the results of an online SANS experiment on a polymerizing C_6MA/DTAB/DDAB/D_2O microemulsion that verifies our assumptions and ideas about how monomer partitioning, micelle size, shape, and number density and particle size distribution evolve throughout the polymerization process.

2. Materials and Methods

DTAB and DDAB, from TCI America with 99+% purity, were used as received. *N*-hexyl methacrylate (C_6MA) (Scientific Polymer Products, 99%) was vacuum distilled and stored under 4 psig of ultrahigh purity nitrogen (<1 ppm O_2) at temperatures below 0 °C for less than 72 h before use. The initiator, 2,2′-azobis(2-amidinopropane) hydrochloride (V50) (Wako Pure Chemical Industries, Ltd., 98.8%) and D_2O (Cambridge Isotopes Laboratories, 99.9%, low-conductivity) were used as received. The microemulsion (375 g) was prepared at a composition similar to that used by Morgan et al.[1] (3.6/8.4/4.4/83.6 wt % DTAB/DDAB/C_6MA/D_2O; 3 g of D_2O reserved for initiator solution) in a 500 mL water-jacketed reactor assembled inside a glovebag purged five times with nitrogen. After removal from the glovebag, the reactor headspace was sparged with ultrahigh purity nitrogen at 6 psig for 10 min before stirring the microemulsion to remove residual oxygen. The reactor contents were heated to 65 ± 1.5 °C and the polymerization was initiated by injecting 3.00 g of a V50/D_2O solution to give an overall concentration of 2.62 × 10^{-5} M, which equals a 1.5 × 10^{-4} weight ratio of V50 to monomer.

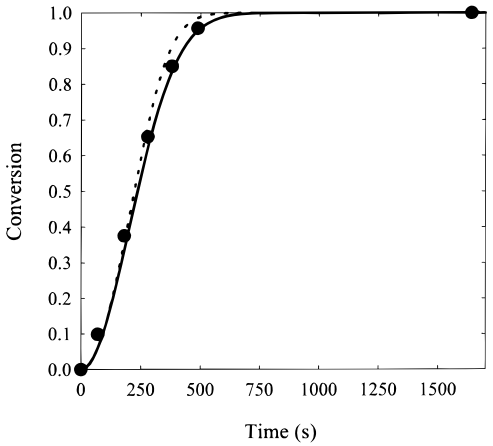

Figure 1. Experimental conversion vs time for the C_6MA microemulsion polymerization studied using online SANS. Solid and dashed lines are the kinetic model predictions where the monomer concentration at the locus of polymerization is related to the conversion using a linear relationship and eq 6, respectively.

Ninety seconds after injection of the initiator solution, the microemulsion became noticeably bluish as the monomer swollen micelles are initiated and grow to form larger polymer particles. This short induction period indicates that only a very low concentration of oxygen, which retards or inhibits free-radical reactions, was present in the microemulsion. This procedure accurately reproduces the experimental kinetic data obtained by Morgan et al.[1] The microstructure of the polymerizing microemulsion was studied as a function of conversion by periodically flowing some of the reactor contents to both a specially designed SANS cell and to an online Anton Paar DMA 60/602W densimeter to monitor conversion. The SANS cell consists of a thermostated aluminum block with fused-quartz windows and has a large, tilted vase-shaped, sample cross section to permit free drainage of the cell contents. The sample is 1.95 mm thick and was held at 65 ± 1 °C. This online densimetry/SANS procedure avoids complications associated with sample quenching and manual filling of conventional SANS cells. Densimetry and SANS both show that the reaction is quenched upon removal from the reactor. The observed quenching of the reaction is possibly due to the high oxygen permeability of the platinum cured silicone tubing (Cole-Parmer) used.

The vapor pressure of C_6MA was measured from 18 to 30 °C using a static still[7] to estimate the enthalpy of vaporization (49 kJ/mol) via the Clausius−Clapeyron equation. The density of C_6MA (850.6 kg/m^3) at 60 °C was measured using an Anton Paar DMA 60/602W densimeter. From these measurements, the solubility parameter of C_6MA was estimated to be 7.5 (cal/cm^3)$^{1/2}$.

The partial molar volume of DDAB (810 Å^3) used in the SANS modeling was measured by adding DDAB to a stock solution of 9.1 wt % DTAB in H_2O. Over the range of 0−0.15 mole ratio of DDAB to DTAB, the molar volume of the solution at 60 °C was linear with respect to the mole fraction of DDAB.

3. Experimental Kinetics and Molecular Weight Distributions

The reaction kinetics (Figure 1) are described accurately by the kinetic model of Morgan et al.[1] using appropriate values for the initial monomer concentration (c_o = 1.91 M), bulk monomer concentration (M_o = 0.28 M), initiator concentration ([I] = 2.62 × 10^{-5} M),

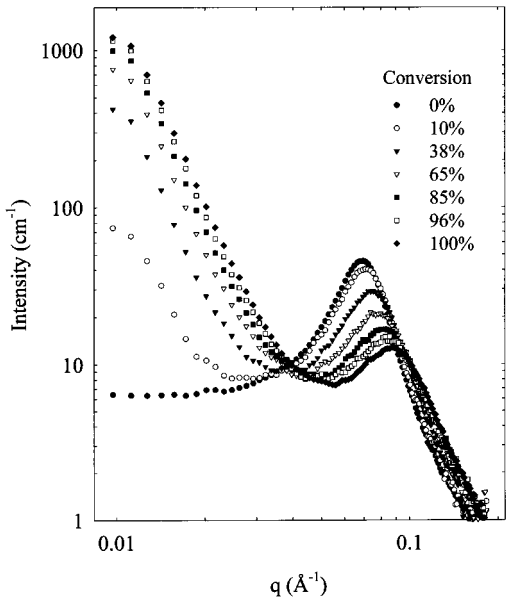

Figure 2. SANS spectra of the polymerizing C_6MA/DTAB/DDAB/D_2O microemulsion as a function of monomer conversion.

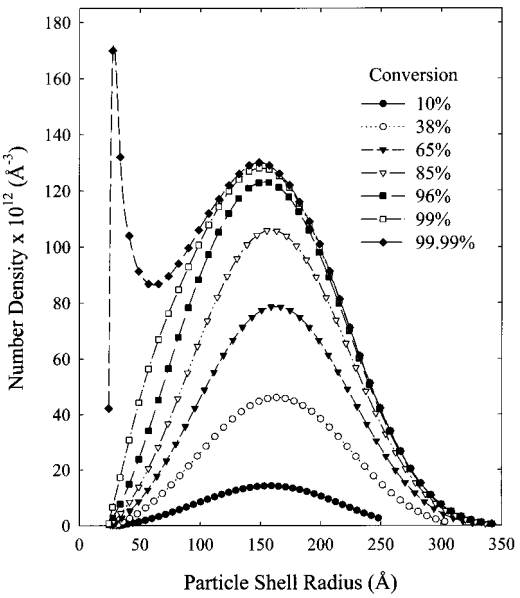

Figure 3. Model calculations of the discretized particle size distribution within the polymerizing microemulsion at monomer conversions corresponding to those measured using online SANS. Particle radii shown are calculated using eq 11 and includes the surfactant/monomer shell surrounding the polymer core.

initiator dissociation constant ($k_d = 5.87 \times 10^{-5}$ s^{-1} at 65 °C[8]), and propagation rate constant ($k_p = 1190$ M^{-1} s^{-1}, estimated from Arrhenius parameters of four other methacrylates[9]).

Attempts to measure the molecular weight distributions of microemulsion polymerized C_6MA, using size exclusion chromatography (SEC) coupled with low-angle laser light scattering (LALLS) and refractive index (RI) detectors, suggest that the polymers formed have very low polydispersities (~1.1) and high molecular weights exceeding 1×10^7. However, plots of ln M_w vs V_e (elution volume) were always nonlinear and highly concave upward at larger V_e. This nonlinearity is indicative of long-chain branching or column adsorption.[10] Consequently, interpretation of the SEC/LALLS/RI data is not straightforward, and the measured polydispersities are probably incorrect since the LALLS detector is highly biased toward the higher molecular weight components. Nevertheless, the weight average molecular weights measured using SEC/LALLS/RI are still reliable and have been verified independently by Polymer Laboratories (Amherst, MA). The weight average molecular weight of poly-C_6MA microemulsion polymerized using the procedure described previously at 60 °C is 1.9×10^7.

4. Qualitative Interpretation of the SANS Experiment

SANS spectra for the polymerizing microemulsion at various levels of conversion are shown in Figure 2. The important features to note are the gradual increase in intensity at low q and the shift of the micelle interaction peak toward higher q with increasing conversion. The increase in intensity at low q can be attributed to an increase in either average particle size or particle number density or both. The accompanying shift of the micelle interaction peak toward higher q indicates that the average intermicellar distance is decreasing due to changes in micelle size or in the effective intermicellar interaction potential. During the polymerization process, the amount of water and ionic surfactant in the microemulsion remains constant. Therefore, the changes in the effective intermicellar interaction potential or distance should mainly be due to a decrease in the average micelle size. The quantitative SANS modeling results presented below are consistent with this qualitative analysis.

It is important to note the gradual and steady shift of the SANS spectra as the microemulsion polymerizes. If the thermodynamic modeling results described previously for the microemulsion polymerization of styrene (wherein the micelles are depleted of monomer at low conversions) are applicable, then an abrupt shift in the SANS spectra at the early stages of polymerization should have been observed. The steady movement of the high q part of the spectra shows that the micelles are being gradually depleted of monomer throughout the polymerization process. This indicates that the other limit of complete segregation of monomer and polymer is likely to be the case. The quantitative analysis of the SANS spectra that follows allows validation of this assumption and verifies the form of the particle size distribution (Figure 3) predicted (paper 1) using a self-consistent microstructure model.

5. Modeling of the SANS Spectra

Prior SANS measurements of similar microemulsions and of mixed DTAB/DDAB micellar solutions[2,3] show that both the empty and monomer swollen micelles are prolate spheroids with aspect ratios of approximately 2. This asymmetry, combined with the complicated electrostatic interparticle interactions and the inherent polydispersity of the latex makes it necessary to use an approximate model in fitting the SANS data.

Assuming that the ellipsoidal micelles are free to rotate, the intermicellar interactions can be approximated by the excluded volume interactions arising from effective hard spheres.[11] With this approximation, the analytical equations of Vrij[12] for the absolute scattering intensity from a multicomponent mixture of hard spheres

Table 1. Modeling and SANS Fitting Results

		fitting parameters				calculated parameters			particle size distribution	
conversion (%)	time (s)	minor shell radius (Å)[b]	shell aspect ratio[b]	effective hard sphere ratio	χ^2	number of surfactants per micelle	micelle number density (Å^{-3}) × 10^6	particle number density (Å^{-3}) × 10^9	average radius (Å)	standard deviation (Å)
0	0	28.6 (31)	2.1 (1.8)	1.6	49	220	1.03			
10	70	27.4	2.2	1.6	94	209	1.08	0.31	155	47
38	180	25.6	2.1	1.6	34	176	1.25	0.90	164	53
65	278	22.9	2.3	1.7	17	152	1.43	1.45	165	55
85	380	21.8	2.2	1.7	16	131	1.61	1.92	163	56
96	488	20.7	2.3	1.7	9	120	1.75	2.29	158	57
100[a]	1641[a]	20.2 (19.5)	2.2 (2.1)	1.6	12	109	1.95	2.52	132	69

[a] Modeled at 99% conversion. [b] Numbers in parentheses from Lusvardi et al. using 60 °C SANS spectra.

can be used to fit the SANS spectra with a limited number of adjustable parameters. Furthermore, since the number density ratio of micelles to particles is approximately 1000, the effective hard sphere radius used for the micelles accounts for essentially all the interactions within the mixed colloidal system, and the effective hard sphere radii of the polymer particles can be set as their actual radii. A microstructure model for microemulsion polymerization that is consistent with the kinetic and particle size distribution models described previously is used in calculating the single particle scattering amplitude factors of the micelles and polymer particles. This microstructure model is summarized below and described in detail in the Appendix.

Following Lusvardi et al.,[3] the micelles are modeled as core−shell prolate spheroids. The micelle cores consist of a uniform mixture of surfactant tails and C_6MA molecules while their shells are a uniform mixture of surfactant ammonium headgroups, bromide counterions, associated waters of hydration, and one methylene group from each surfactant tail. The parameters used to describe the micelles are the minor shell radius (r_{MS}), the shell aspect ratio (A_{MS}), and the shell thickness (d_{ST}). Interactions are described by an effective hard sphere radius ($=E_{HS}\ r_{MS}$). These four parameters (r_{MS}, A_{MS}, d_{ST}, E_{HS}) together with the mass balances outlined in the appendix are used to fit model spectra to the SANS spectrum measured at zero conversion. The fitted value of d_{ST} (4.0 Å) is in good agreement with the value of 3.7 Å obtained by Lusvardi et al.[3] using a different set of SANS spectra. In subsequent fitting of the SANS spectra of the polymerizing microemulsions, d_{ST} is held fixed at 4.0 Å.

The polydisperse polymer particles are assumed to consist of a spherical polymer core surrounded first by an inner shell of monomer and surfactant tails and then by an outer shell of surfactant headgroups, bromide counterions, associated water of hydration, and one methylene group from each surfactant tail. Following the kinetic model assumptions, the inner shell of the particles and the core of the micelles have identical compositions. Similarly, the outer shell of the particles and shell of the micelles are assigned identical compositions and thickness. The particle size distribution model derived in paper 1 (eq 29) for transfer-controlled exit is used to describe the evolving particle population. For purposes of calculation, the polymer core size distribution is discretized into 40 radii ($R_{PC,i}$). The density of the polymer core is set equal to the bulk C_6MA polymer density[13] of 1007 kg/m^3. The chain transfer constant (k_{tr}) for C_6MA was not measured, but based on tabulated values for comparable methacrylates[13] at 60 °C, it is estimated to be 0.01 M^{-1} s^{-1}.

Figure 3 shows the predicted discretized particle outer-shell radius distribution up to the maximum particle size at various conversions. Since the model of paper 1 assumes continuous particle nucleation, short chains and small particles are formed toward the end of the reaction. Consequently, at very high conversions (>99%), a secondary peak in the distribution at smaller particle sizes (∼30 Å) becomes more evident. Even though the number of small particles continues to increase at conversions >99%, the changes in the corresponding SANS spectra are negligible. These small particles formed at high conversions contain low molecular weight polymer and so are essentially the same size as the monomer depleted micelles.

The parameters obtained from SANS data fitting after smearing the model spectra[14] ($\Delta\lambda/\lambda = 0.10$) and minimizing the χ^2 statistic are shown in Table 1. The SANS data are fitted using a constant background of 0.5 cm^{-1} obtained from separate experiments[3] while k_{tr} and d_{ST} are fixed at 0.01 M^{-1} s^{-1} and 4.0 Å respectively. Although r_{MS}, A_{MS}, and E_{HS} are used as adjustable parameters, r_{MS} and A_{MS} are not independently adjustable since they must satisfy a mass balance constraint described in the appendix (eq 7). Thus, there are effectively only two independently adjustable parameters used in fitting the SANS spectra of the polymerizing microemulsion.

Figure 4 shows a comparison between model and experimental SANS spectra at four conversion levels. As expected, the low q region of the model SANS spectrum is insensitive to the values of d_{ST} and the adjustable parameters, r_{MS}, A_{MS}, and E_{HS} that describe the micelles. At lower conversions, there are deviations between the experimental and model SANS spectra in the low q region. Fitting the 10% conversion SANS spectra using k_{tr} as an additional adjustable parameter results in insignificant changes in χ^2 and k_{tr} from 94.3 to 93.7 and from 0.0100 to 0.0104 M^{-1} s^{-1} respectively. However, the deviations between the model and experimental SANS spectra can be accounted for by experimental errors in conversion measurement which have a constant absolute error of approximately 5%. The effect of this error is shown in Figure 5 where the experimental nominal 10% conversion SANS spectra is compared with the calculated model SANS spectra of the microemulsion at 2%, 5%, and 10% conversion. At higher conversions, where the relative error in conversion measurement is smaller, the model fit to the SANS spectra improves significantly.

The effective hard sphere ratio (E_{HS}) and micelle shell aspect ratio (A_{MS}) are approximately constant and range from 1.58 to 1.67 and from 2.08 to 2.33, respectively. As expected from the qualitative discussion above, the

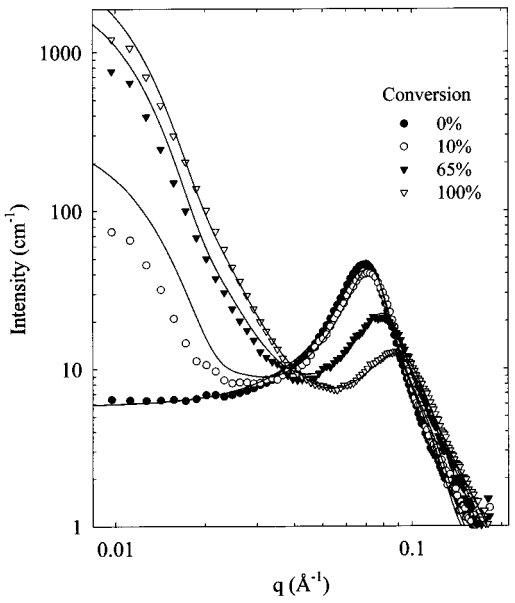

Figure 4. SANS model fitting results using the particle size distributions shown in Figure 3. Numerical fitting results are tabulated in Table 1.

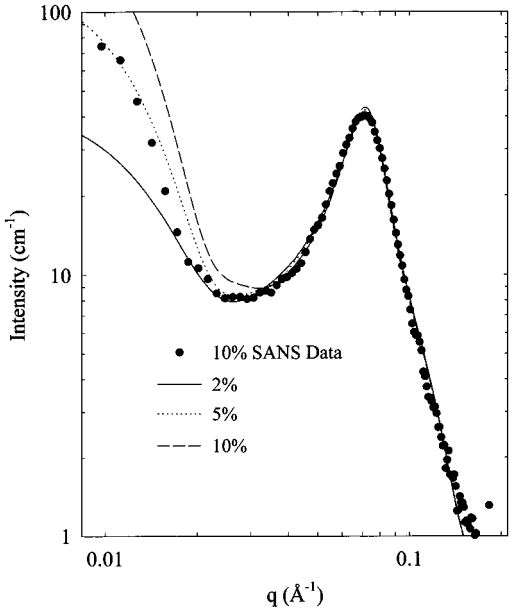

Figure 5. Sensitivity analysis of the SANS experiment with respect to conversion. Points show experimental SANS spectra obtained at 10% conversion as measured using densimetry. Dashed, dotted, and solid lines are fitted model SANS spectra assuming 2%, 5%, and 10% conversion, respectively.

micelle minor shell radius (r_{MS}) decreases gradually and steadily from 28.6 to 20.2 Å with increasing conversion. Conservation of headgroup volumes requires that this decrease in micelle size be accompanied by a corresponding decrease in surfactant aggregation number from 220 to 109 and an increase in micelle number density. As mentioned previously, there are approximately 1000 micelles per polymer particle, and even at full conversion, the interfacial area of the particles comprises only ~5% of the total interfacial area.

A final check of the validity of this SANS fitting procedure comes from comparing the size and shape of the micelles estimated using this procedure with the micelle dimensions determined by Lusvardi et al.[2,3] using different SANS measurements and more sophisticated SANS models. As shown in Table 1, the micelle dimensions of the unpolymerized microemulsion estimated from these two separate studies are in good agreement. At the end of the polymerization, the system contains 4.4 wt % of poly-C_6MA particles and monomer-free mixed micelles of DTAB and DDAB surfactants with a total concentration of 0.37 M and DTAB mole fraction of 0.78. The estimated dimensions of these monomer-free mixed micelles are also in good agreement with those obtained by Lusvardi et al.[2] for mixed micelles of DTAB and DDAB at a total concentration of 0.4 M and DTAB mole fraction of 0.8 in the absence of polymer particles.

6. Discussion

Microemulsion polymerization is an effective technique for making small latex particles. The particle size distributions as predicted by the model at different monomer conversions are shown in Figure 3. In contrast to conventional emulsion polymerization, the particle size distribution has an approximately constant and small average particle size with a standard deviation that increases slightly with conversion. As shown previously, the model SANS spectra calculated using this particle size distribution model are also consistent with the measured SANS spectra within conversion measurement errors. For the fully polymerized microemulsion, where the monomer conversion can be determined exactly, the model SANS spectra calculated using the particle size distribution model is in quantitative agreement with the measured SANS spectra. Furthermore, even though the SANS model has effectively two adjustable parameters that describe the monomer swollen micelles, the value of these do not influence the scattering intensity calculated for low q values that is characteristic of the polymer particles.

Thermodynamic modeling of the microemulsion polymerization of styrene suggests that the monomer partitions mainly in the polymer particles formed at low conversions.[5] However, for C_6MA, the opposite is suggested by experimental kinetic data as well as qualitative and quantitative analysis of the SANS results. Micelles swollen with C_6MA monomer are depleted gradually throughout the polymerization. These two opposing observations can be rationalized based on the relative solubility of the monomer in the polymer or in the hydrocarbon surfactant tails. The solubility parameter of styrene monomer,[15] 9.3 (cal/cm^3)$^{1/2}$, is almost equal to that of polystyrene,[13] 9.1 (cal/cm^3)$^{1/2}$, but is significantly different from that of the surfactant tails, which likely have solubility parameters in the range of 7−8 (cal/cm^3)$^{1/2}$, as typical of aliphatic hydrocarbons.[15] In contrast, C_6MA has a solubility parameter of 7.5 (cal/cm^3)$^{1/2}$, as determined from vapor pressure measurements, which essentially matches the hydrocarbon solubility parameters, while poly-C_6MA has a much higher solubility parameter[13] of 8.6 (cal/cm^3)$^{1/2}$.

Recent SANS studies[16−18] on dilute (5 wt %), emulsion polymerized polystyrene latexes suggest a particle morphology consisting of a polymer core and a monomer-rich shell,[19−23] where the thickness of the monomer-rich shell increases with the ratio of the radius of gyration of the polymer to the particle diameter. This core−shell morphology has been rationalized by the extreme hy-

drophobicity of the polymer that leads to a reduction in the number of accessible chain conformations inside the confined spherical geometry, i.e., a "repulsive-wall" effect.[24−26] The small particle size and high molecular weight of microemulsion polymerized latexes suggest that this repulsive-wall effect may also be an important factor during microemulsion polymerization. At the low micelle concentrations characteristic of emulsion polymerization systems, this entropic contribution affects only the homogeneity of the polymer particles. However, for microemulsion polymerization systems, this repulsive-wall effect may be a significant factor that not only favors polymer-core/monomer-rich shell particle morphologies but also affects monomer partitioning between the micelles and polymer particles. Thus microemulsion polymerization processes can lead to different polymer structures or configurations.

The chain transfer constants to monomer or polymer have not been measured for C_6MA. However tabulated values for methyl methacrylate[13] suggest that the chain transfer constants to monomer or polymer are comparable. Since the monomer does not significantly swell the polymer during the microemulsion polymerization of C_6MA, the polymer concentration in the particles is high even at very low conversions. Therefore, chain transfer to polymer may be important and the polymer formed may have a higher degree of branching than would be expected if the monomer swells the polymer. Polymer branching would in turn result in more compact and globular conformations and could be another factor promoting the formation of a polymer core/monomer shell particle morphology during polymerization. Indeed, as mentioned previously, accurate analysis of the full molecular weight distributions of microemulsion polymerized poly-C_6MA using SEC/LALLS/RI has been hampered by complications that are possibly due to long-chain branching.

7. Conclusions

The SANS spectra of the polymerizing C_6MA/DTAB/DDAB/D_2O microemulsion show that the monomer does not significantly swell the polymer particles. The assumption of a polymer-core/monomer-rich shell polymer particle morphology where the monomer concentration in the shell of the particles is equal to that in the core of the monomer swollen micelles is consistent with both kinetic and SANS data. An important consequence of the segregation between C_6MA monomer and polymer is the high polymer concentration at the locus of polymerization throughout the reaction that could lead to significant long-chain branching.

The analytical equation for the particle size distribution derived from the kinetic model quantitatively describes the SANS spectra of the completely polymerized microemulsion. This quantitative agreement between model and experimental SANS spectra is achieved with two independent adjustable parameters that describe the effective excluded radius and size of the micelles. Furthermore, the size of the micelles in the completely polymerized microemulsion obtained using this SANS model is in excellent agreement with that obtained from independent SANS measurements of the corresponding monomer-free surfactant solution.

Acknowledgment. We acknowledge the support of the National Institute of Standards and Technology, U.S. Department of Commerce, in providing the facilities used for experiments performed there. The assistance of K. Lusvardi, L. Ryan, D. Iampietro, and S. Kline in performing the neutron scattering experiments is gratefully acknowledged. Financial support was provided by the Delaware Research Partnership and by a National Science and Engineering Research Council of Canada Fellowship to C.C.C.

8. Appendix

Several mass balances can be made to relate the volumes of monomer, polymer, and surfactant. These constrain the three adjustable parameters (r_{MS}, A_{MS}, E_{HS}) used in fitting the SANS spectra. Following Lusvardi et al.,[3] the micelle cores are assumed to consist of a uniform mixture of surfactant tails and C_6MA molecules. The micelle shells are assumed to be a uniform mixture of surfactant ammonium headgroups with 80% of the bromide counterions, associated waters of hydration (1 and 4 respectively for the ammonium headgroups and bromide counterion[27]), and one methylene group from each surfactant tail. The total surfactant tail (V_{TST}) and shell (V_{TSS}) volume fractions are

$$V_{TST} = (N_{DTAB} + 2N_{DDAB})(V_{CH_3} + 10V_{CH_2}) \quad (2)$$

$$V_{TSS} = N_{DTAB}V_{NC_3} + N_{DDAB}V_{NC_2} + (N_{DTAB} + 2N_{DDAB})V_{CH_2} + N_{TS}[0.8V_{Br} + (1 + 4(0.8)V_{D_2O})] \quad (3)$$

The average tail and shell volumes are

$$\bar{V}_{ST} = \frac{V_{TST}}{N_{TS}} \quad \text{and} \quad \bar{V}_{SS} = \frac{V_{TSS}}{N_{TS}} \quad (4)$$

where N_{DTAB}, N_{DDAB}, and N_{TS} are the individual and total surfactant number densities respectively, and V_{CH_3} (54.3 Å^3), V_{CH_2} (26.9 Å^3), V_{NC_3} (102.3 Å^3), V_{NC_2} (70.6 Å^3), V_{Br} (39.3 Å^3), V_{D_2O} (30.2 Å^3), are the molecular volumes of the CH_3 and CH_2 groups, the DTAB and DDAB headgroups, the bromide counterion, and the solvent, respectively.[27,28] V_{NC_2} was found to be 70.6 Å^3 by subtracting the volume of the surfactant tails and the bromide counterion from the partial molar volume of DDAB (810 Å^3).

The scattering length density of the micelle surfactant shells (ρ_{MS}) is readily calculated as the ratio of the scattering length (calculated in analogy to eq 3) to V_{TSS}. The scattering length density of the micelle core (ρ_{MC}) is

$$\rho_{MC} = \frac{\bar{L}_{ST} + N_{MonS}L_{Mon}}{V_{ST} + N_{MonS}V_{Mon}} \quad (5)$$

where the average surfactant scattering length $\bar{L}_{ST}$ is defined similarly to $\bar{V}_{ST}$ in eq 4, and L_{Mon} and V_{Mon} are the monomer scattering length and molecular volume, respectively. N_{MonS} is the ratio of the number density of monomer (N_{TMon}) to surfactant (N_{TS}). The monomer concentration (C_{Mon}) in the micelle core can be calculated as a function of conversion (f) via

$$C_{Mon} = \frac{N^\circ_{TMon}(1 - f)}{N_{TS}\bar{V}_{ST} + N^\circ_{TMon}(1 - f)V_{Mon}} \quad (6)$$

Here, N°_{TMon} is the initial number density of monomer molecules, and V_{Mon} (332.3 Å^3) is the monomer

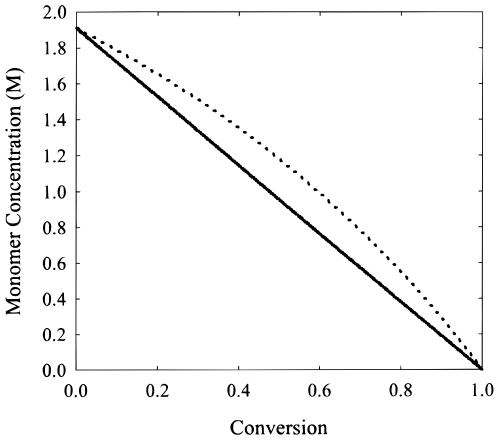

Figure 6. Estimated monomer concentration at the locus of polymerization. The dotted line is the monomer concentration calculated using eq 6 which accounts for the diluting effect of the hydrocarbon surfactant tails. The solid line is the linearized form of eq 6 as used in the kinetic and chain length/particle size distribution models.

molecular volume calculated from the measured bulk density at 60 °C.

The linear decrease in monomer concentration with conversion assumed in the kinetic model, i.e., $c = c_o(1 - f)$, follows if $(1 - f)$ is neglected in the second term in the denominator. In this case, c_o is simply the initial monomer concentration in the micelle cores, and the surfactant tails merely act as diluents. For the molecules and compositions of interest here, the difference between eq 6 and the linearized version used in the kinetic model (see Figure 6) is negligible. Figure 1 also shows the negligible difference between the predicted conversions using the exact expression for the monomer concentration (eq 6) and its linearized version in the kinetic model. Calculation of the rate using eq 6 yields a more complication expression that cannot be used in deriving analytical expressions for the chain length or particle size distributions.

Four parameters are used to describe the micelles. These are the surfactant shell thickness (d_{ST}), the micelle shell aspect ratio (A_{MS}), the micelle minor shell radius (r_{MS}) and an effective hard sphere parameter (E_{HS}). The effective hard sphere radius ($r_{HS} = E_{HS}r_{MS}$), the micelle major shell radius ($R_{MS} = A_{MS}r_{MS}$), the micelle major core radius ($R_{MC} = R_{MS} - d_{ST}$), and the micelle minor core radius ($r_{MC} = r_{MS} - d_{ST}$) are calculated from these parameters. With these micelle core and shell dimensions, the individual micelle (V_M) and micelle shell (V_{MS}) volumes can be used to calculate the number density of micelles (N_M) on the basis of either total micelle volume (V_{TM}) or total micelle shell volume (V_{TMS}).

$$N_M = \frac{V_{TM}}{V_M} = \frac{V_{TMS}}{V_{MS}} \tag{7}$$

The second equality is used as a constraint in the fitting procedure. V_{TM} and V_{TMS} take into account the surfactant adsorbed on the latex particles (N_{TSL}) using the inventories:

$$V_{TM} = (V_{TST} + V_{TSS}) - N_{TSL}(\bar{V}_{ST} + \bar{V}_{SS}) + N_{TMon}V_{Mon} \tag{8}$$

$$V_{TMS} = V_{TSS} - N_{TSL}\bar{V}_{SS} \tag{9}$$

$$N_{TSL} = \sum_{i=1}^{p}(N_{PS,i})(N_{P,i}) \tag{10}$$

$N_{P,i}$ is the number density of particles with polymer core radius $R_{PC,i}$ and $N_{PS,i}$ is the number of adsorbed surfactant molecules on a particle of size i. Calculations are made with the size distribution predicted for a transfer-controlled exit discretized into 40 sizes. The model for the surfactant-coated latex particles consists of a polymer core surrounded by two shells. The inner shell has a composition equal to that of the micelle core, and the outer shell has a composition equal to that of the micelle shell.

The radii of the inner and outer shells ($R_{PIS,i}$ and $R_{POS,i}$) are related by

$$R_{POS,i} = R_{PIS,i} + d_{ST} \tag{11}$$

and the values of the two radii are found by iterating eqs 11−13.

$$R_{PIS,i} = \left[\frac{3}{4\pi}N_{PS,i}(N_{MonS}V_{Mon} + \bar{V}_{ST}) + R_{PC,i}{}^3\right]^{1/3} \tag{12}$$

$$N_{PS,i} = \frac{4\pi}{3V_{SS}}(R_{POS,i}{}^3 - R_{PIS,i}{}^3) \tag{13}$$

If the volumes and compositions of the core and shells of the prolate spheroid micelles and spherical particles are known, the calculation of the corresponding scattering length densities and single particle scattering amplitude factors ($F_i(q)$) is straightforward.[29]

References and Notes

(1) Morgan, J. D.; Lusvardi, K. M.; Kaler, E. W. *Macromolecules* **1997**, *30*, 1897.
(2) Lusvardi, K. M.; Full, A. P.; Kaler, E. W. *Langmuir* **1995**, *11*, 487.
(3) Lusvardi, K. M.; Schubert, K. V.; Kaler, E. W. *Langmuir* **1995**, *11*, 4728.
(4) Gilbert, R. G. *Emulsion Polymerization: A Mechanistic Approach*; Academic Press: San Diego, CA, 1995; p 59.
(5) Guo, J. S.; Sudol, E. D.; Vanderhoff, J. W.; El-Aaser, M. S. *J. Polym. Sci., Polym. Chem. Ed.* **1992**, *30*, 691.
(6) Guo, J. S.; El-Aasser, M. S.; Vanderhoff, J. W. *J. Polym. Sci., Polym. Chem.* **1989**, *27*, 691.
(7) Pividal, K. A.; Birtigh, A.; Sandler, S. I. *J. Chem. Eng. Data* **1992**, *37*, 484.
(8) *V-50*; Wako Pure Chemical Industries, Ltd.: Richmond, VA.
(9) Hutchinson, R. A.; Paquet, D. A.; McMinn, J. H.; Beuermann, S.; Fuller, R. E.; Jackson, C. *DECHEMA Monogr.* **1995**, *131*, 467.
(10) Glockner, G. *Polymer Characterization by Liquid Chromatography*; Elsevier Science Publishers: Amsterdam, 1987.
(11) Hansen, J. P.; McDonald, I. R. *Theory of Simple Liquids*, 2nd ed.; Academic Press: London, 1986; p 450.
(12) Vrij, A. *J. Chem. Phys.* **1979**, *71*, 3267.
(13) *Polymer Handbook*, 3rd ed.; Brandrup, J., Immergut, E. H., Eds.; John Wiley & Sons: New York, 1989; pp II/85, II/88.
(14) Pedersen, J. S.; Posselt, D.; Mortensen, K. *J. Appl. Crystallogr.* **1990**, *23*, 321.
(15) Sandler, S. I. *Chemical and Engineering Thermodynamics*, 2nd ed.; John Wiley & Sons: New York, 1989; p 340.
(16) Yang, S.; Klein, A.; Sperling, L. H. *J. Polym. Sci., Polym. Phys. Ed.* **1989**, *27*, 1649.
(17) Yang, S.; Klein, A.; Sperling, L. H.; Casassa, E. F. *Macromolecules* **1990**, *23*, 4582.
(18) Dabdub, D.; Klein, A.; Sperling, L. H. *J. Polym. Sci., Polym. Phys. Ed.* **1992**, *30*, 787.
(19) Grancio, M. R.; Williams, D. J. *J. Polym. Sci., A-1* **1970**, *8*, 2733.

(20) Grancio, M. R.; Williams, D. J. *J. Polym. Sci., A-1* **1970**, *8*, 2617.
(21) Wessling, R. A.; Gibbs, D. S. *J. Macromol. Sci., Chem.* **1973**, *A7*, 647.
(22) Keusch, P.; Prince, J.; Williams, D. J. *J. Macromol. Sci., Chem.* **1973**, *A7*, 623.
(23) Keusch, P.; Williams, D. J. *J. Polym. Sci., Polym. Chem. Ed.* **1973**, *11*, 143.
(24) Casassa, E. F. *Polym. Lett.* **1967**, *5*, 773.
(25) Casassa, E. F.; Tagami, Y. *Macromolecules* **1969**, *2*, 14.
(26) de Gennes, P. G. *Macromolecules* **1981**, *14*, 1637.
(27) Hayter, J. B.; Penfold, J. *Colloid Polym. Sci.* **1983**, *261*, 1022.
(28) Berr, S. S.; Coleman, M. J.; Marriott, R. R.; Johnson, J. S. *J. Phys. Chem.* **1986**, *90*, 6492.
(29) Chen, S. H. *Annu. Rev. Phys. Chem.* **1986**, *37*, 351.

MA971718A